Original Article

Tao-Hong-Si-Wu Decoction ameliorates steroid-induced avascular necrosis of the femoral head by regulating the HIF-1α pathway and cell apoptosis

Jian Wu[1,*], Li Yao[1], Bing Wang[1], Zhen Liu[2], Keyong Ma[1]

[1] *Department of Joint Surgery, The First People's Hospital of Lianyungang, Lianyungang, Jiangsu, China;*
[2] *Department of Rehabilitation, The First People's Hospital of Lianyungang, Lianyungang, Jiangsu, China.*

Summary	The aim of this study was to corroborate the hypothesis that Tao-Hong-Si-Wu Decoction (THSWD) affects steroid-induced avascular necrosis of the femoral head (SANFH) by regulating the hypoxia-inducible factor 1α (HIF-1α) pathway. Forty-eight New Zealand rabbits were randomly divided into a normal control group (NC group), a model group (SANFH group), a THSWD group, and a dimethyloxalylglycine group (DMOG group). Rabbits in the SANFH group were injected with both horse serum and methylprednisolone. Rabbits in the THSWD group were gavaged with THSWD in addition to receiving the same treatment as the SANFH group. Rabbits in the DMOG group were injected with extra DMOG in conjunction with the same treatment as the SANFH group. Rabbits in the NC group received the same amount of normal saline. Eight weeks after steroid treatment, the femoral heads of rabbits were removed to examine HIF-1α, vascular endothelial growth factor (VEGF), caspase-3, and bcl-2. Results indicated that THSWD significantly promoted the expression of HIF-1α and VEGF in the femoral head tissue of rabbits and markedly inhibit the apoptosis of osteocytes, chondrocytes, and bone marrow cells. In addition, THSWD suppressed caspase-3 expression and induced bcl-2 expression in femoral head tissues. In conclusion, THSWD can suppress SANFH by regulating the HIF-1α pathway and cell apoptosis.

Keywords: Tao-Hong-Si-Wu Decoction, avascular necrosis of the femoral head, HIF-1α, VEGF, caspase-3, bcl-2

1. Introduction

Steroid-induced avascular necrosis of the femoral head (SANFH) is an aseptic and ischemic condition that may result from long-term use of glucocorticoids. This condition is primarily characterized by the necrosis of bone marrow and trabecular bones (*1*). As suggested by a Chinese epidemiologic study, SANFH accounts for approximately 24.1% of all cases of osteonecrosis of the femoral head (ONFH) (*2*). Thus far, the mechanism underlying SANFH has not been not clear (*3*), but

the general consensus is that several pathways may interrupt the bone microcirculation process and affect the supply of essential nutrients. As a result, deaths of both osteocytes and fat cells may occur, resulting in further damage to bone structures (*4*). As SANFH progresses, bone collapse and osteoarthritis may also occur, and patients are likely to experience intolerable pain and ankylosis (*4,5*). SANFH affects patients with the condition directly and it also has a long-term impact on the health care system (*6*). An estimated four out of five patients may experience femoral head collapse if osteonecrosis occurs due to inappropriate treatment (*1*).

Most approaches used to preserve the joint focus on preventing collapse primarily by supporting the underlying subchondral bone (*7*) and there is debate as to whether these approaches are effective over the long term (*8*). Since a large proportion of patients with SANFH are adolescents who usually need additional surgery, identifying molecular and genetic pathways

that are associated with SANFH may assist clinicians to determine the optimal timing of surgery and to devise preventive interventions for articular surface collapse (*4*).

Hypoxia-inducible factors (HIFs) are a class of DNA-binding transcription factors that is able to activate a series of hypoxia-related genes under certain circumstances and trigger an adaptive response in order to decrease oxygen tension. Researchers have identified approximately 100 HIFs, including vascular endothelial growth factor (VEGF), hemexygenase-1, and glucose transporter protein-1 (*9*). As previous studies have suggested, VEGF promotes the development of new blood vessels and activated VEGF stimulates angiogenesis, erythropoiesis, and cell proliferation and survival (*10,11*). Furthermore, Riddle *et al.* reported that VEGF plays significant roles in angiogenic-osteogenic coupling in the process of osteanagenesis as a target of HIF-1α (*12*). A study by Li *et al.* found that deferoxamine stimulates angiogenesis and bone repair in SANFH by up-regulating the expression of HIF-1α (*8*). All of these findings indicate that activated HIF-1α pathways have positive effects on angiogenesis, osteanagenesis, and cell protection. Therefore, HIF-1α pathways could presumably be targeted in patients with SANFH. Caspase-3 is an apoptosis-related protein that may cleave cellular substrates and lead to apoptosis (*13*). Recent studies have suggested that the pathophysiology of SANFH is likely to be associated with the apoptosis of osteoblasts and osteocytes, which is mediated by nitric oxide (NO) (*14,15*). In addition, Weinstein *et al.* noted the marked apoptosis of osteocytes in specimens obtained from patients with SANFH (*16*).

Tao-Hong-Si-Wu Decoction (THSWD) is a traditional Chinese medication that consists of four basic herbs: Radix Rehmanniae Praeparata (shu di huang), Radix Angelicae Sinensis (dang gui), Rhizoma Ligustici (Chuan xiong), and Radix Paeoniae Alba (bai shao). THSWD also contains two additional ingredients, Semen Prunus and Flos Carthami Tinctorii. A wide range of benefits of THSWD have been identified since its introduction, including stimulation of blood circulation, neuroprotection, and facilitation of angiogenesis (*17-19*). A combination of a recombinant tissue-type plasminogen activator and THSWD resulted in a decreased infarct size, it stimulated cerebral blood circulation, and it enhanced neuron function in patients who had suffered a cerebral embolic stroke (*20*). THSWD has been used to treat rabbits in a model of SANFH, resulting in reduced blood viscosity, increased regeneration of local micro-vessels, improved local blood supply, and facilitation of the recovery of the necrotic femoral head (*21,22*). THSWD appears to be closely associated with regulation of HIF-1α, and HIF-1α is reported to prevent the occurrence of SANFH (*1,23*). However, few systematic studies have consolidated the aforementioned findings, and whether THSWD affects SANFH *via* the HIF-1α signaling pathway is still debated.

The current study sought to explore the effects of THSWD in a model of SANFH by detecting the level of VEGF expression and clarifying the role of the HIF-1α pathway. This study also detected the rate of cell apoptosis and it examined the level of expression of the apoptosis-related proteins caspase-3 and Bcl-2 in order to determine whether THSWD influences cell apoptosis in a model of SANFH. This study represents an intriguing approach that links HIF-1α to SANFH and it also reveals potential clues to managing patients with SANFH in clinical practice.

2. Materials and Methods

2.1. *Lentivirus transduction and creation of a model of SANFH*

A fragment containing HIF-1α was cloned into a pCDH vector. This vector was, together with other packaging plasmids, co-transfected into cells using the Lipofectamine LTX kit (Invitrogen, CA), and the viral particles therein were collected 48 h after transfection.

A total of 48 healthy New Zealand rabbits weighing between 2.0 and 2.5 kg were housed at the Experimental Animal Center of The First People's Hospital of Lianyungang at a temperature of $25 \pm 3°C$ and all rabbits were fed normally. All experimental protocols were approved by the Medical Animal Studies Committee of The First People's Hospital of Lianyungang, China.

Rabbits ate and drank freely with a normal 12 h-light and 12 h-dark cycle. After rabbits were given an initial adaptation period of seven days, they were randomly divided into 4 groups: a SANFH group (*n* = 12), a THSWD group (*n* = 12), a vector group (*n* =12), and an HIF-1α group (*n* = 12). Rabbits in the SANFH group were injected with horse serum (Sigma, USA) *via* the ear vein at a dose of 10 mg/kg. After 3 weeks, horse serum was injected again *via* the ear vein at a decreased dose of 6 mg/kg. After 2 weeks, methylprednisolone (Sigma) was injected into rabbits intraperitoneally at a daily dose of 45 mg/kg for 3 consecutive days. Penicillin was also injected intraperitoneally accompanied with the injection of hormones in order to prevent infection. Rabbits in the THSWD group were gavaged with THSWD at a concentration of 0.75 g/mL, 20 µg/g once a day in addition to receiving the same treatment as the SANFH group. Rabbits in the vector group were injected with Lentivirus, and an empty vector (5.5×10^{11} vp/mL, 25 µL per side) was injected into the collapsed portion of the femoral head in addition to receiving the same treatment as the SANFH group. Rabbits in the HIF-1α group were injected with Lentivirus, and an HIF-1α fragment (5.5×10^{11} vp/mL, 25 µL per side) was injected into the collapsed portion of the femoral head in addition to receiving the same treatment as the SANFH group.

No rabbits died during creation of the model and

Table 1. HIF-1α, VEGF, and β-actin primers for RT-PCR

Gene	Forward	Reverse	Length
HIF-1α	5'-GCTTGCTCATCAGTTGCC-3'	5'-GCCTTCATTTCATCTTCAATATCC-3'	706 bp
VEGF	5'-TGCACCCACGACAGAAGGGGA-3'	5'-TCACCGCCTTGGCTTGTCACAT-3'	360 bp
β-actin	5'-CCCATTGAACACGGCATT-3'	5'-GGTACGACCAGAGGCATACA-3'	250 bp

HIF-1α: Hypoxia-inducible factor 1α; VEGF: vascular endothelial growth factor; RT-PCR: reverse transcription-polymerase chain reaction.

SANFH was verified using hematoxylin and eosin (HE) staining. Rabbits in each group were sacrificed after eight weeks and their femoral heads were examined using both RT-PCR and immunohistochemical analysis.

2.2. Immunohistochemistry (IHC)

IHC was performed to detect the expression of HIF-1α, VEGF, caspase-3, and bcl-2 proteins. IHC was performed in triplicate for each sample and femoral head tissues in the NC control group served as controls. All tissue samples were incubated with primary antibodies against HIF-1α (1:500), VEGF (1:400), caspase-3 (1:500), and bcl-2 (1:500) overnight at 4°C and then incubated with a secondary antibody biotinylated with goat anti-mouse IgG (1:900) for 30 minutes. Phosphate buffer saline (PBS) solutions served as the negative controls in order to replace the primary antibodies and all antibodies were purchased from Santa Cruz. Six random fields were chosen for each sample (× 200) in order to record the number of positive cells. Another 10 random fields were then chosen and positive staining was determined based on the integrated optical density (IOD). IHC results were analyzed by two independent researchers using the software Image-Pro Plus 6.0.

2.3. RNA isolation and RT-PCR

Total RNA from tissues was isolated using the TRIzol reagent (Invitrogen, Germany) according to the manufacturer's instructions. The ReverTra Ace qPCR RT Kit (Toyobo, Japan) was used to transcribe total RNA into cDNA, and RT-PCR was performed with the THUNDERBIRD SYBR® qPCR Mix (Toyobo, Japan) using the CFX96 Touch Real-Time PCR Detection System (Bio-Rad). The corresponding primer sequences are listed in Table 1. The level of expression of the target gene was normalized to that of β-actin and was calculated using the $2^{-\Delta\Delta CT}$ method. The corresponding experiment was replicated three times.

2.4. Intra-artery ink perfusion

Intra-artery ink perfusion assay was performed to visualize and assess the blood supply in the femoral head of rats. Rats were intraperitoneally administered pentobarbital sodium and then the inferior vena cava and abdominal aorta were immediately exposed and ligated. One tube used to infuse ink was inserted into the distal abdominal aorta and another tube for drainage was inserted into the inferior vena. Heparinized saline (25,000 units in 250 mL 0.9% sodium chloride) was used to wash the inferior vena, and then the abdominal aorta was infused with 10% gelatin/Indian ink (20 g gelatin in 100 mL Indian ink and 100 mL water) using a pressure of 90 mmHg. The above procedures were continued until the toes and lower legs were uniformly black. Samples were harvested and stained using HE. The ratio of perfusion was calculated with the software Image-Pro Plus 6.0 (Media Cybernetics, Silver Spring, MD), and the ratio of perfusion was defined as the area of the inked artery with respect to the area of the entire artery.

2.5. Quantification of microvessel density (MVD)

MVD was used to determine the state of angiogenesis, which was quantified by IHC with anti-CD31 antibody as previous described (*24*). A single endothelial cell or endothelial cell cluster that was clearly separated from adjacent microvessels was considered to be a microvessel.

2.6. Transferase-mediated dUTP nick end labeling (TUNEL) assay

A TUNEL detection kit (Promega, China) was used to evaluate apoptosis according to the manufacturer's instructions. Cells that were colored brown or that contained brown-yellow nuclei or brown-yellow granules in their cytoplasm were classified as TUNEL-positive cells. TUNEL-positive cells were observed under a fluorescent microscope (Nikon, Japan) at 200×. The corresponding rate of apoptosis was calculated as the number of TUNEL-positive cells divided by the total number of cells. Calculations were obtained by three independent researchers.

2.7. Statistical analysis

All statistical analysis was performed with the software SPSS 21.0 (Chicago, USA). Continuous data are expressed as the mean ± standard deviation (S.D.). A *t*-test or one-way analysis of variance (ANOVA) was used to compare groups and a *p*-value of less than 0.05 was considered to indicate statistical significance.
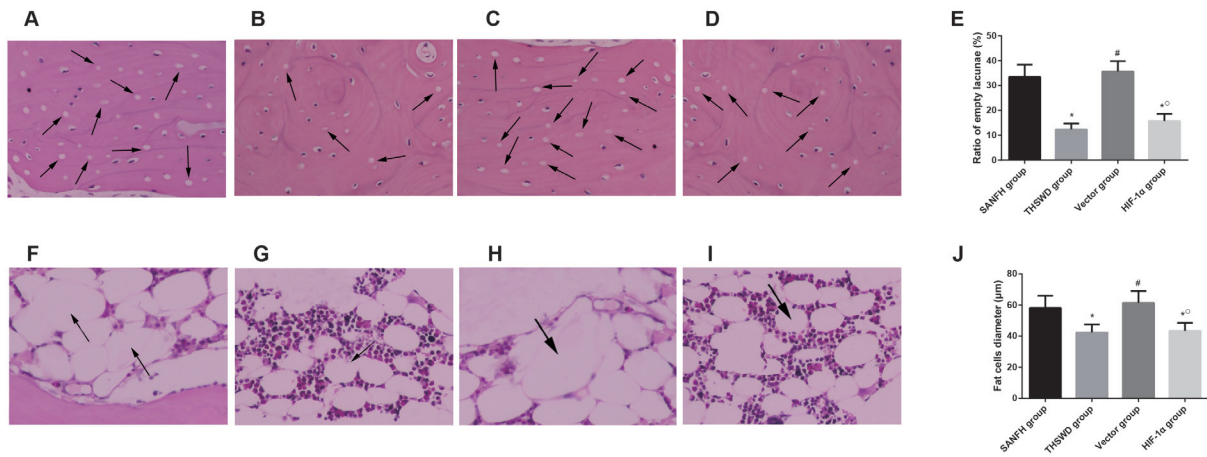
Figure 1. Histopathological observations (200×). Empty lacunae were observed in the SANFH group **(A)**, THSWD group **(B)**, vector group **(C)**, and HIF-1α group **(D)**. Comparison of the ratio of empty lacunae among the four groups **(E)**. The diameter of fat cells was measured in the marrow of the SANFH group **(F)**, THSWD group **(G)**, vector group **(H)**, and HIF-1α group **(I)**. Comparison of the diameter of fat cells among the four groups **(J)**. SANFH: avascular necrosis of the femoral head, THSWD: Tao-Hong-Si-Wu Decoction. Data are presented as the mean ± S.D. *$p < 0.05$ *vs.* the SANFH group, #$p < 0.05$ *vs.* the THSWD group, °$p < 0.05$ *vs.* the vector group.
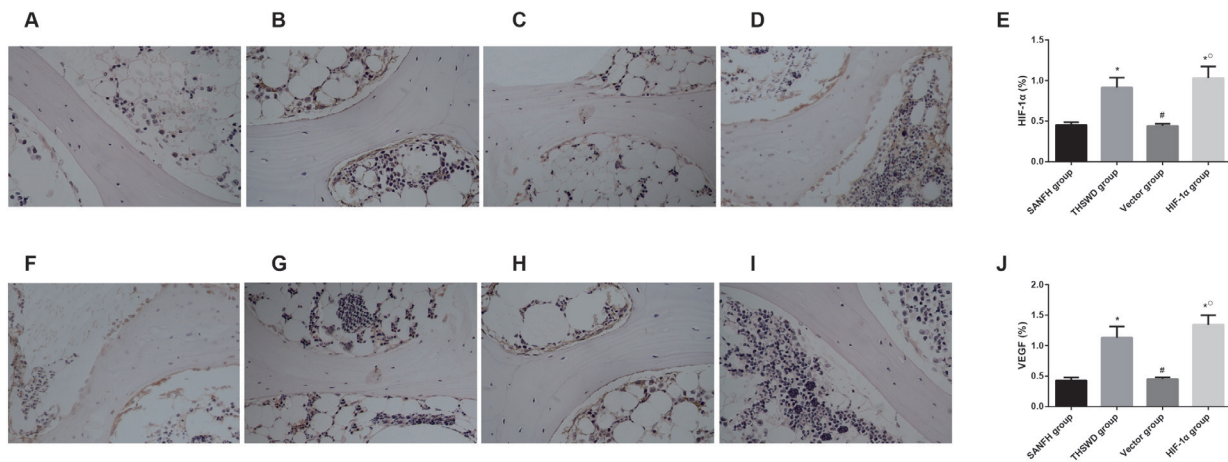

Figure 2. Immunohistochemical staining of HIF-1α and VEGF (200×). Immunohistochemical staining of HIF-1α in the SANFH group **(A)**, THSWD group **(B)**, vector group **(C)**, and HIF-1α group **(D)**. Semi-quantitative analysis of HIF-1α in the four groups **(E)**. Immunohistochemical staining of VEGF in the SANFH group **(F)**, THSWD group **(G)**, vector group **(H)**, and HIF-1α group **(I)**. Semi-quantitative analysis of VEGF in the four groups **(J)**. Data are presented as the mean ± S.D. *$p < 0.05$ *vs.* the SANFH group, #$p < 0.05$ *vs.* the THSWD group, °$p < 0.05$ *vs.* the vector group.

3. Results

3.1. *THSWD and HIF-1α played protective roles in the process of SANFH*

As shown in Figure 1A-E, rats in the SANFH and vector groups displayed obvious osteonecrosis, which was evident as pyknosis and empty lacunae in bone cells. The ratio of empty lacunae in the THSWD and HIF-1α groups was significantly lower than that in the SANFH and vector groups ($p < 0.05$). In addition, the cellular structure of some fat cells collapsed, whereas the diameter of fat cells in the THSWD and HIF-1α groups was significantly smaller than the diameter of those cells in the SANFH and vector groups ($p < 0.05$, Figure 1F-J).

3.2. *THSWD promoted HIF-1α and VEGF expression in femoral head tissues*

Levels of HIF-1α and VEGF expression were measured using IHC and RT-PCR in order to assess whether THSWD was able to affect the HIF-1α pathway. As suggested by the eight-week IHC analysis (Figure 2), the HIF-1α group exhibited higher levels of HIF-1α and VEGF expression than the other groups. The THSWD group had increased levels of HIF-1α and VEGF expression in comparison to the SANFH and vector groups ($p < 0.05$). Similarly, RT-PCR results indicated that the level of expression of HIF-1α mRNA in the THSWD and HIF-1α groups was markedly higher than that in the SANFH and vector groups ($p < 0.05$; Figure 3A). A similar trend in VEGF expression is shown in

Figure 3B ($p < 0.05$). Therefore, results indicated that the HIF-1α pathway is regulated by THSWD.

3.3. *Angiogenesis was regulated by THSWD and HIF-1α*

The results of intra-arterial ink perfusion are shown in Figure 4. Few capillaries that formed a sparse network
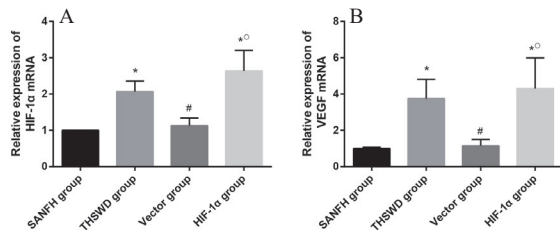
were identified in the medullary cavity of rats in the SANFH and vector groups. The perfusion ratios in the THSWD and HIF-1α groups were significantly higher than those in the SANFH and vector groups ($p < 0.05$). MVD is shown in Figure 5, indicating immunostaining for CD31. Both the THSWD and HIF-1α groups exhibited significantly larger numbers of microvessels in subchondral bone in comparison to the SANFH and vector groups ($p < 0.05$).

3.4. *THSWD inhibited the apoptosis of osteocytes, chondrocytes, and bone marrow cells*

The average rate of apoptosis in the four groups was calculated once the corresponding treatment had been administered for eight weeks. Apoptosis of osteocytes, chondrocytes, and bone marrow cells was examined. As shown in Figure 6, the number of TUNEL-positive cells in the THSWD and HIF-1α groups was significantly lower than the number of those cells in the SANFH and vector groups ($p < 0.05$). These findings suggested that

Figure 3. Levels of expression of HIF-1α (A) and VEGF (B) mRNA were measured in femoral head tissues using RT-PCR. Data are presented as the mean ± S.D. *$p < 0.05$ *vs.* the SANFH group, #$p < 0.05$ *vs.* the THSWD group, °$p < 0.05$ *vs.* the vector group.
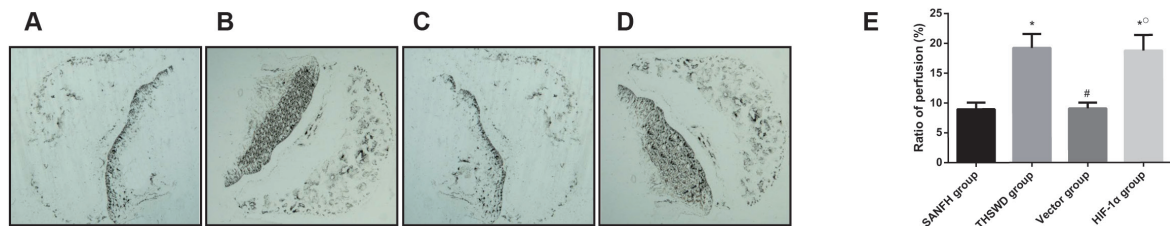

Figure 4. Results of intra-arterial ink perfusion in the SANFH group (A), THSWD group (B), vector group (C), and HIF-1α group (D), and a comparison of the perfusion ratio among the four groups (200×). Data are presented as the mean ± S.D. *$p < 0.05$ *vs.* the SANFH group, #$p < 0.05$ *vs.* the THSWD group, °$p < 0.05$ *vs.* the vector group.
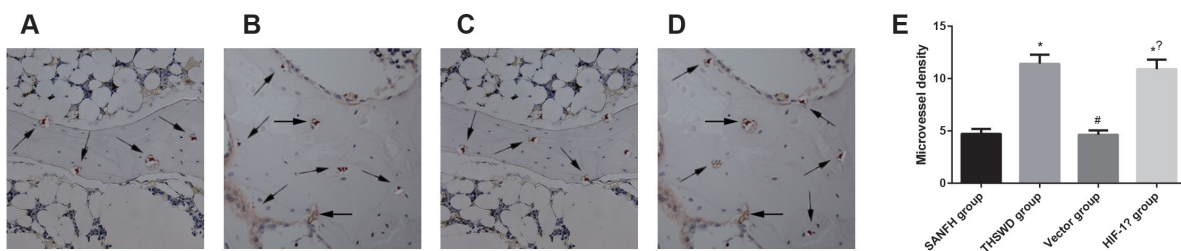

Figure 5. Immunohistochemical staining using antibodies against CD31 in the SANFH group (A), THSWD group (B), vector group (C), and HIF-1α group (D) and a comparison of microvessel density among the four groups (200×). Data are presented as the mean ± S.D. *$p < 0.05$ *vs.* the SANFH group, #$p < 0.05$ *vs.* the THSWD group, °$p < 0.05$ *vs.* the vector group
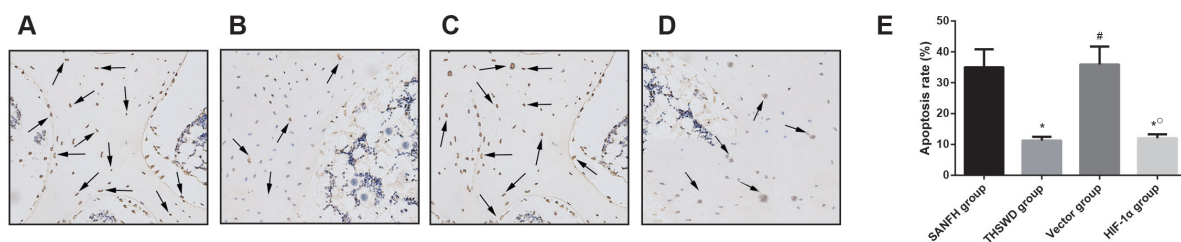

Figure 6. The apoptosis of osteocytes, chondrocytes, and bone marrow cells in the SANFH group (A), THSWD group (B), vector group (C), and HIF-1α group (D) was determined with a TUNEL assay, and the quantitative results were analyzed (200×). Data are presented as the mean ± S.D. *$p < 0.05$ *vs.* the SANFH group, #$p < 0.05$ *vs.* the THSWD group, °$p < 0.05$ *vs.* the vector group.
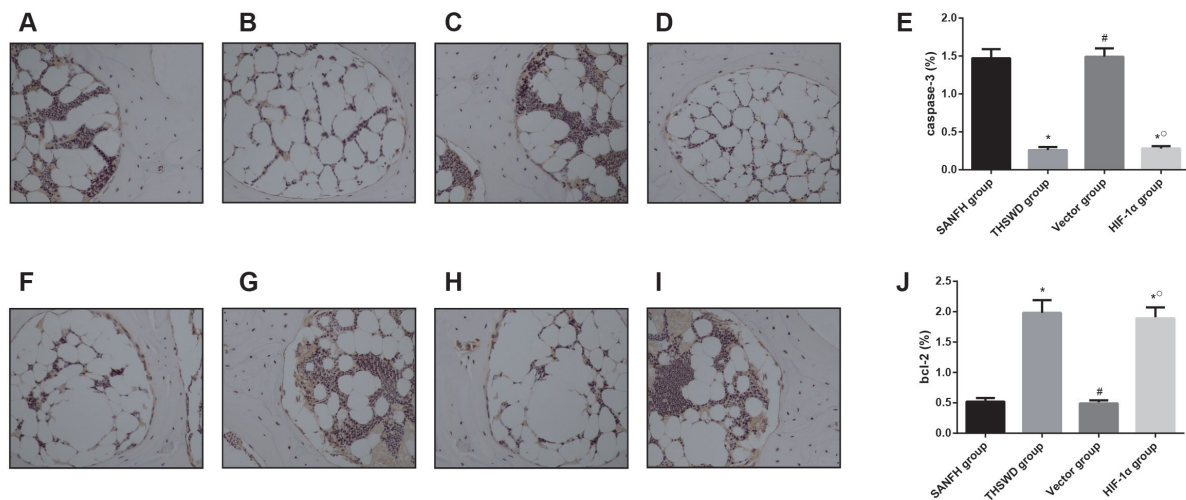
Figure 7. Immunohistochemical staining of caspase-3 and bcl-2 (200×). Immunohistochemical staining of caspase-3 in the SANFH group **(A)**, THSWD group **(B)**, vector group **(C)**, and HIF-1α group **(D)**. Semi-quantitative analysis of caspase-3 in the four groups **(E)**. Immunohistochemical staining of bcl-2 in the SANFH group **(F)**, THSWD group **(G)**, vector group **(H)**, and HIF-1α group **(I)**. Semi-quantitative analysis of bcl-2 in the four groups **(J)**. Data are presented as the mean ± S.D. *$p < 0.05$ *vs.* SANFH group, #$p < 0.05$ *vs.* THSWD group, °$p < 0.05$ *vs.* vector group.

both THSWD and HIF-1α can suppress early apoptosis in steroid-associated osteonecrosis.

3.5. THSWD inhibited caspase-3 expression and induced bcl-2 expression in femoral head tissues

IHC was performed to assess the levels of expression of apoptosis-related proteins such as caspase-3 and bcl-2 in femoral head tissues. Figure 7A-E shows that immunoreactivity to caspase-3 was weak in the THSWD and HIF-1α groups but significantly stronger in the SANFH and vector groups ($p < 0.05$). The THSWD and HIF-1α groups exhibited strong immunoreactivity to bcl-2 while the SANFH and vector groups exhibited relatively weak immunoreactivity ($p < 0.05$, Figure 7F-J). Therefore, THSWD and HIF-1α were able to suppress the progression of SANFH by influencing the expression of apoptosis-related proteins.

4. Discussion

SANFH is a condition often found in young and middle-aged populations, and excessive or long-term usage of steroids accounts for most cases of SANFH (*25*). Steroid hormones regulate the metabolism of sugar, fat, and proteins and also affect oxidative stress, cell proliferation, and apoptosis (*26*). The current study attempted to establish a link between THSWD and HIF-1α/VEGF pathways in order to clarify whether THSWD is able to regulate the apoptosis of bone cells.

Although the mechanisms SANFH are unclear, the consensus view is that the final result of SANFH is an interruption of bone microcirculation (*27*), mainly through disruption of angiogenesis and limiting of the penetration of new vessels into necrotic bone (*1*). Regular angiogenesis is thus crucial to ameliorating SANFH,

since angiogenesis is closely correlated with increased circulation of oxygen and nutrients in bone tissues (*28*). HIF-1α is a key regulatory factor that restores the intracellular oxygen concentration, and HIF-1α has been found to play a critical role in manipulating angiogenesis in stem cells (*29*). The significance of HIF-1α is also evident from the fact that administration of ethyl 3,4-dihudroxybenzoate (EDHB) deters the progression of SANFH because it inhibits the functioning of HIF prolyl hydroxylase and it stabilizes HIF-1α expression (*1,30,31*). A target gene of HIF-1α, VEGF, also plays a major role in encouraging the angiogenesis-osteogenesis coupling process (*32-34*). VEGF improves angiogenesis by activating a variety of signal pathways. One such pathway is the MEK/ERK pathway, which is crucial to the proliferation of endothelial cells (*35*).

In addition, steroids may accelerate osteonecrosis by facilitating the apoptosis of osteoblasts and osteocytes, thereby partially contributing to bone cell death (*14,36-38*). Bcl-2 and caspase-3 are typical apoptosis-related factors. Bcl-2 was found to be up-regulated and caspase-3 was found to be down-regulated during the development of SANFH (*39*). Intriguingly, HIF-1α appears to regulate numerous pro-apoptotic proteins (*e.g.* BNIP3 and NOXA) and anti-apoptotic proteins (*e.g.* Bcl-2, Bcl-xl and Bid) as well (*40,41*). Since the HIF-1α signaling pathway has been found to be involved in regulation of the morphology/function of bone cells and osteoblasts (*42*), HIF-1α presumably plays a major role in the progression of SANFH.

THSWD was first described in the traditional Chinese medical text "YiZongJinJian" (*The Golden Mirror of Medical Orthodoxy*). In response to the negative effects of SANFH, THSWD excels at limiting the aggregation of platelets, increasing blood viscosity, and altering blood stasis (*43,44*). Three components of THSWD, *i.e.*

danggui, chuan xiong, and bai shao, have been found to improve microcirculation and to facilitate microvessel regeneration. These effects are specifically evident in the form of increased blood/plasma viscosity, repair/limited aggregation of blood cells, and a decrease in plasma fibrinogen levels (*45*). THSWD is adept at restoring a necrotic femoral head, and this restoration starts at the interface between the necrotic bone and normal bone. The new bone tissues that form cover the surface of necrotic bone trabeculae and thereby form a dense mass. Fibrous granulation tissues form within this mass and bone resorption spreads to the necrotic portion of bone. Despite restoration reaching a certain stage, collapse of the femoral head can occur because of poor blood circulation (*46*). A key potential action of THSWD is that it may improve blood flow in microcirculation, and this action has been enhanced by modifying both HIF-1α and TNF-α (*23*). These contentions ultimately imply that THSWD might promote osteogenesis and angiogenesis by elevating HIF-1α.

The current study used the traditional Chinese medicine THSWD to specifically treat SANFH, and this study filled a gap in research with solid evidence that THSWD molecularly modified HIF/VEGF signaling to ameliorate symptoms of SANFH. Moreover, this study lifted the mysterious veil surrounding traditional Chinese medicine and it suggested that THSWD is beneficial to patients with SANFH by facilitating angiogenesis and suppressing cell apoptosis. These findings suggest that certain molecules within THSWD might play a crucial role in alleviation of micro-circulatory disturbances, and extraction of these molecules should be the next priority. The extracts can be concentrated and made into pills, since pills would be a convenient and highly efficient form of administration.

In conclusion, levels of HIF-1α and VEGF expression were elevated when THSWD was given. THSWD inhibited the apoptosis of bone cells and the transference of HIF-1α in order to regulate the transcription of VEGF. These findings suggest that THSWD might ameliorate SANFH by regulating HIF-1α signaling and inhibiting the apoptosis of bone cells. Nevertheless, these conclusions should be investigated further in clinical trials in order to justify use of THSWD as an effective treatment for SANFH.

References

1. Fan L, Li J, Yu Z, Dang X, Wang K. Hypoxia-inducible factor prolyl hydroxylase inhibitor prevents steroid-associated osteonecrosis of the femoral head in rabbits by promoting angiogenesis and inhibiting apoptosis. PloS One. 2014; 9:e107774.
2. Cui L, Zhuang Q, Lin J, Jin J, Zhang K, Cao L, Lin J, Yan S, Guo W, He W, Pei F, Zhou Y, Weng X. Multicentric epidemiologic study on six thousand three hundred and ninety five cases of femoral head osteonecrosis in China. Int Orthop. 2016; 40:267-276.
3. Fotopoulos V, Mouzopoulos G, Floros T, Tzurbakis M. Steroid-induced femoral head osteonecrosis in immune thrombocytopenia treatment with osteochondral autograft transplantation. Knee Surg Sports Traumatol Arthrosc. 2015; 23:2605-2610.
4. Powell C, Chang C, Gershwin ME. Current concepts on the pathogenesis and natural history of steroid-induced osteonecrosis. Clin Rev Allergy Immunol. 2011; 41:102-113.
5. Alves EM, Angrisani AT, Santiago MB. The use of extracorporeal shock waves in the treatment of osteonecrosis of the femoral head: A systematic review. Clin Rheumatol. 2009; 28:1247-1251.
6. Kerachian MA, Seguin C, Harvey EJ. Glucocorticoids in osteonecrosis of the femoral head: A new understanding of the mechanisms of action. J Steroid Biochem Mol Biol. 2009; 114:121-128.
7. Jones LC, Hungerford DS. Osteonecrosis: Etiology, diagnosis, and treatment. Curr Opin Rheumatol. 2004; 16:443-449.
8. Li J, Fan L, Yu Z, Dang X, Wang K. The effect of deferoxamine on angiogenesis and bone repair in steroid-induced osteonecrosis of rabbit femoral heads. Exp Biol Med (Maywood). 2015; 240:273-280.
9. Masoud GN, Li W. HIF-1alpha pathway: Role, regulation and intervention for cancer therapy. Acta Pharm Sin B. 2015; 5:378-389.
10. Shen X, Wan C, Ramaswamy G, Mavalli M, Wang Y, Duvall CL, Deng LF, Guldberg RE, Eberhart A, Clemens TL, Gilbert SR. Prolyl hydroxylase inhibitors increase neoangiogenesis and callus formation following femur fracture in mice. J Orthop Res. 2009; 27:1298-1305.
11. Tsai CC, Chen YJ, Yew TL, Chen LL, Wang JY, Chiu CH, Hung SC. Hypoxia inhibits senescence and maintains mesenchymal stem cell properties through down-regulation of E2A-p21 by HIF-TWIST. Blood. 2011; 117:459-469.
12. Riddle RC, Khatri R, Schipani E, Clemens TL. Role of hypoxia-inducible factor-1alpha in angiogenic-osteogenic coupling. J Mol Med (Berl). 2009; 87:583-590.
13. Xu X, Wen H, Hu Y, Yu H, Zhang Y, Chen C, Pan X. STAT1-caspase 3 pathway in the apoptotic process associated with steroid-induced necrosis of the femoral head. J Mol Histol. 2014; 45:473-485.
14. Calder JD, Buttery L, Revell PA, Pearse M, Polak JM. Apoptosis – a significant cause of bone cell death in osteonecrosis of the femoral head. J Bone Joint Surg Br. 2004; 86:1209-1213.
15. Youm YS, Lee SY, Lee SH. Apoptosis in the osteonecrosis of the femoral head. Clin Orthop Surg. 2010; 2:250-255.
16. Zhang C, Zou YL, Ma J, Dang XQ, Wang KZ. Apoptosis associated with Wnt/beta-catenin pathway leads to steroid-induced avascular necrosis of femoral head. BMC Musculoskelet Disord. 2015; 16:132.
17. Han L, Ji Z, Chen W, Yin D, Xu F, Li S, Chen F, Zhu G, Peng D. Protective effects of tao-Hong-si-wu decoction on memory impairment and hippocampal damage in animal model of vascular dementia. Evid Based Complement Alternat Med. 2015; 2015:195835.
18. Li L, Yang N, Nin L, Zhao Z, Chen L, Yu J, Jiang Z, Zhong Z, Zeng D, Qi H, Xu X. Chinese herbal medicine formula tao hong si wu decoction protects against cerebral ischemia-reperfusion injury *via* PI3K/Akt and

the Nrf2 signaling pathway. J Nat Med. 2015; 69:76-85.

19. Xu X, Wang S, Chen W, Chen G. Effects of taohong siwu decoction II in the chick chorioallantoic membrane (CAM) assay and on B16 melanoma in mice and endothelial cells ECV304 proliferation. J Tradit Chin Med. 2006; 26:63-67.

20. Yen TL, Ong ET, Lin KH, Chang CC, Jayakumar T, Lin SC, Fong TH, Sheu JR. Potential advantages of Chinese medicine Taohong Siwu Decoction (桃红四物汤) combined with tissue-plasminogen activator for alleviating middle cerebral artery occlusion-induced embolic stroke in rats. Chin J Integr Med. 2014. DOI: 10.1007/s11655-014-1847-x

21. Qi ZX, Du CB. Local microcirculation changes in rabbits with glucocorticoid-induced avascular necrosis of femoral head following Taohong Siwudecoction treatment. Journal of Clinical Rehabilitative Tissue Engineering Research. 2008; 12:2104-2107.

22. Qi ZX, Cao Y. Comparative study of different methods for the treatment of glucocorticoid induced necrosis of the femoral head. China Journal of Orthopaedics and Traumatology. 2002;2:17-18. (in Chinese)

23. Wu CJ, Chen JT, Yen TL, Jayakumar T, Chou DS, Hsiao G, Sheu JR. Neuroprotection by the Traditional Chinese Medicine, Tao-Hong-Si-Wu-Tang, against Middle Cerebral Artery Occlusion-Induced Cerebral Ischemia in Rats. Evid Based Complement Alternat Med. 2011; 2011:803015.

24. Weidner N, Semple JP, Welch WR, Folkman J. Tumor angiogenesis and metastasis – correlation in invasive breast carcinoma. N Engl J Med. 1991; 324:1-8.

25. Wang J, Kalhor A, Lu S, Crawford R, Ni JD, Xiao Y. iNOS expression and osteocyte apoptosis in idiopathic, non-traumatic osteonecrosis. Acta Orthop. 2015; 86:134-141.

26. Yu Q, Guo W, Shen J, Lv Y. Effect of glucocorticoids on lncRNA and mRNA expression profiles of the bone microcirculatory endothelial cells from femur head of Homo sapiens. Genom Data. 2015; 4:140-142.

27. Mont MA, Cherian JJ, Sierra RJ, Jones LC, Lieberman JR. Nontraumatic osteonecrosis of the femoral head: Where do we stand today? A Ten-Year Update. J Bone Joint Surg Am. 2015; 97:1604-1627.

28. Stegen S, van Gastel N, Carmeliet G. Bringing new life to damaged bone: The importance of angiogenesis in bone repair and regeneration. Bone. 2015; 70:19-27.

29. Mutijima E, De Maertelaer V, Deprez M, Malaise M, Hauzeur JP. The apoptosis of osteoblasts and osteocytes in femoral head osteonecrosis: Its specificity and its distribution. Clin Rheumatol. 2014; 33:1791-1795.

30. Baay-Guzman GJ, Bebenek IG, Zeidler M, Hernandez-Pando R, Vega MI, Garcia-Zepeda EA, Antonio-Andres G, Bonavida B, Riedl M, Kleerup E, Tashkin DP, Hankinson O, Huerta-Yepez S. HIF-1 expression is associated with CCL2 chemokine expression in airway inflammatory cells: Implications in allergic airway inflammation. Respir Res. 2012; 13:60.

31. Chu PW, Beart PM, Jones NM. Preconditioning protects against oxidative injury involving hypoxia-inducible factor-1 and vascular endothelial growth factor in cultured astrocytes. Eur J Pharmacol. 2010; 633:24-32.

32. Zhang W, Yuan Z, Pei X, Ma R. *In vivo* and *in vitro* characteristic of HIF-1alpha and relative genes in ischemic femoral head necrosis. Int J Clin Exp Pathol. 2015; 8:7210-7216.

33. Drescher W, Schlieper G, Floege J, Eitner F. Steroid-related osteonecrosis – an update. Nephrol Dial Transplant. 2011; 26:2728-2731.

34. Weinstein RS, Wan C, Liu Q, Wang Y, Almeida M, O'Brien CA, Thostenson J, Roberson PK, Boskey AL, Clemens TL, Manolagas SC. Endogenous glucocorticoids decrease skeletal angiogenesis, vascularity, hydration, and strength in aged mice. Aging Cell. 2010; 9:147-161.

35. Yin D, Liu Z, Peng D, Yang Y, Gao X, Xu F, Han L. Serum Containing Tao-Hong-Si-Wu Decoction Induces Human Endothelial Cell VEGF Production *via* PI3K/Akt-eNOS Signaling. Evid Based Complement Alternat Med. 2013; 2013:195158.

36. Weinstein RS, Jilka RL, Parfitt AM, Manolagas SC. Inhibition of osteoblastogenesis and promotion of apoptosis of osteoblasts and osteocytes by glucocorticoids. Potential mechanisms of their deleterious effects on bone. J Clin Invest. 1998; 102:274-282.

37. Samara S, Dailiana Z, Chassanidis C, Koromila T, Papatheodorou L, Malizos KN, Kollia P. Expression profile of osteoprotegerin, RANK and RANKL genes in the femoral head of patients with avascular necrosis. Exp Mol Pathol. 2014; 96:9-14.

38. Tsuji M, Ikeda H, Ishizu A, Miyatake Y, Hayase H, Yoshiki T. Altered expression of apoptosis-related genes in osteocytes exposed to high-dose steroid hormones and hypoxic stress. Pathobiology. 2006; 73:304-309.

39. Tian L, Dang XQ, Wang CS, Yang P, Zhang C, Wang KZ. Effects of sodium ferulate on preventing steroid-induced femoral head osteonecrosis in rabbits. J Zhejiang Univ Sci B. 2013; 14:426-437.

40. Chen MH, Ren QX, Yang WF, Chen XL, Lu C, Sun J. Influences of HIF-lalpha on Bax/Bcl-2 and VEGF expressions in rats with spinal cord injury. Int J Clin Exp Pathol. 2013; 6:2312-2322.

41. Sowter HM, Ratcliffe PJ, Watson P, Greenberg AH, Harris AL. HIF-1-dependent regulation of hypoxic induction of the cell death factors BNIP3 and NIX in human tumors. Cancer Res. 2001; 61:6669-6673.

42. Zuo GL, Zhang LF, Qi J, Kang H, Jia P, Chen H, Shen X, Guo L, Zhou HB, Wang JS, Zhou Q, Qian ND, Deng LF. Activation of HIFa pathway in mature osteoblasts disrupts the integrity of the osteocyte/canalicular network. PloS One. 2015; 10:e0121266.

43. Han L, Peng DY, Xu F, Wang N, Liu D, Li YB, Tan QL. Study on antithrombotic effects of Taohong Siwu decoction. Journal of Anhui TCM College. 2010; 29:47-49. (in Chinese)

44. Han L, Xu F, Zhang XB, Xu J, Dai M, Peng DY, Liu QY. The experimental researches of blooding-quickening and stasis-transforming actions of TaoHong Siwu decoction. Journal of Anhui TCM College. 2007; 26:36-38. (in Chinese)

45. Liu JG, Shi DZ. Study of Chinese Herbal Drugs in Affecting Hemorheology Promoting Blood Circulation and Removing Blood Stasis. Chin J Hemorheol. 2004;133-137. (in Chinese)

46. Brody AS, Strong M, Babikian G, Sweet DE, Seidel FG, Kuhn JP. John Caffey Award paper. Avascular necrosis: Early MR imaging and histologic findings in a canine model. AJR Am J Roentgenol. 1991; 157:341-345.